

Modeling of Kink-Effect in RF Behaviour of GaN HEMTs using ASM-HEMT Model

Sheikh Aamir Ahsan*, Sudip Ghosh*, Sourabh Khandelwal† and Yogesh Singh Chauhan*

*Nanolab, Dept. of Electrical Engineering, Indian Institute of Technology Kanpur, India

†Department of Electrical Engineering and Computer Science, University of California, Berkeley, USA

Email: ahsan@iitk.ac.in, chauhan@iitk.ac.in

Abstract—In this paper, a physics-based compact model is reported that captures the kink-effect observed in S_{22} for Al-GaN/GaN HEMTs. The presence of this kink in the Smith-plot of S_{22} severely affects the design of the output matching network for amplifiers based on these devices which calls for a precise consideration of this effect. The kink-effect originates due to the ambivalent nature of the output impedance of the intrinsic device, wherein it changes its nature from a low frequency series-RC network to a high frequency parallel-RC network, giving rise to a kink at the frequency where the contours corresponding to low and high frequency approximations intersect each other. The output impedance is a complicated function of the various intrinsic elements of the device small signal model, and all the device intrinsic characteristics in our model arise from a physics-based framework, therefore, making multi-bias validation of the kink-behaviour with measured data possible with sufficient ease.

Keywords—GaN HEMTs; S_{22} ; kink-effect; modeling

I. INTRODUCTION

Gallium Nitride (GaN) High Electron Mobility Transistors (HEMTs) are being thoroughly investigated for RF and microwave applications due to the phenomenal material properties of GaN such as wide bandgap, high electron saturation velocity etc. [1], [2]. It has been observed that there exists a kink in the Smith-plot of the scattering parameter (S_{22}) for microwave transistors. Previous studies carried out on this phenomenon have thoroughly investigated the reason for this anomalous behaviour [3–5]. The following points summarize the extract of their analysis regarding the kink-effect:

- 1) The kink originates due to the anomalous nature of the output impedance (Z_{out}), which manifests itself as a series-RC network at low-frequency and a parallel-RC network at high-frequency. The low and high frequency approximations of Z_{out} follow constant resistance ($r + \frac{1}{j\omega C}$) and constant conductance ($g + j\omega C$) contours respectively, leading to emergence of a kink at a frequency which represents the point of intersection of the two contours.
- 2) The effect is purely due to the intrinsic device and the extrinsic parasitic elements of the device only affect the shape of kink [6].
- 3) The intrinsic elements of the device small signal model determine the value of Z_{out} . S_{22} , being a strong function of Z_{out} , therefore gets influenced by variation in the intrinsic device characteristics such as the transconductance (g_m), capacitances (C_{gs} , C_{gd} and C_{ds}) etc.
- 4) Increasing g_m and C_{gd} cause the kink to become more pronounced whereas an increase in C_{gs} shifts the kink towards the open circuit load on the Smith-

chart. However, the kink-effect diminishes upon increasing C_{ds} .

Crupi *et al.* proposed a technique to quantify the strength and thereby get a deeper insight of the kink-effect. Moreover, they demonstrated a model that reproduces this kink behaviour in S_{22} [5]. However, their core calculations i.e. the drain current, intrinsic charges etc. were based on a look-up table (LUT) model [7]. The limitation that a LUT based model is faced with is that it is strongly dependent on interpolation functions to compute values for operating conditions for which the data is missing. Furthermore, LUT based models are limited in usage when it comes to scalability.

Since GaN based HEMTs, in general, inherently exhibit superior g_m as against transistors from GaAs and Si based technologies, they tend to show prominence of the kink-effect in S_{22} . As a consequence, the design of broadband output matching networks for RF power amplifiers based on GaN HEMTs tends to get complicated. A compact model that very well captures this feature as well as how this behaviour changes with different operating bias conditions, different device geometries etc. is highly desirable if we are to use such a device in the large signal operation at microwave frequencies. In this paper, we present a physics-based model that accurately captures the kink-effect in S_{22} observed in GaN devices.

II. ASM-HEMT MODEL

The Advanced SPICE Model for GaN High Electron Mobility Transistors (ASM-HEMT) is a physics-based model in which closed form expressions for drain current (I_d) and intrinsic charges ($Q_{g,s,d}$) are derived in terms of surface-potential (ψ) [8–12]. Realistic device effects such as self-heating, trapping effects, access region resistances etc. are incorporated into the model to realise a more realistic device [11]. The bias dependence of the device performance is handled by the model by a bias dependent value of ψ which in turn is an analytical function of the Quasi-Fermi level (E_F) [8]. The ASM-HEMT Model is a potential candidate for getting standardized by the Compact Model Coalition (CMC) [13].

III. DC CHARACTERISTICS AND SMALL SIGNAL MODEL

Fig. 1 shows the DC-IV fits for a $10 \times 90 \mu\text{m}$ device. The model accurately reproduces the impact of various realistic behavioural nuances within the device. Apart from giving precise fits for I_d - V_d and I_d - V_g , the model is accurate enough in predicting the corresponding derivatives g_m and g_{ds} respectively, which are instrumental in determining the aforementioned kink in S_{22} .

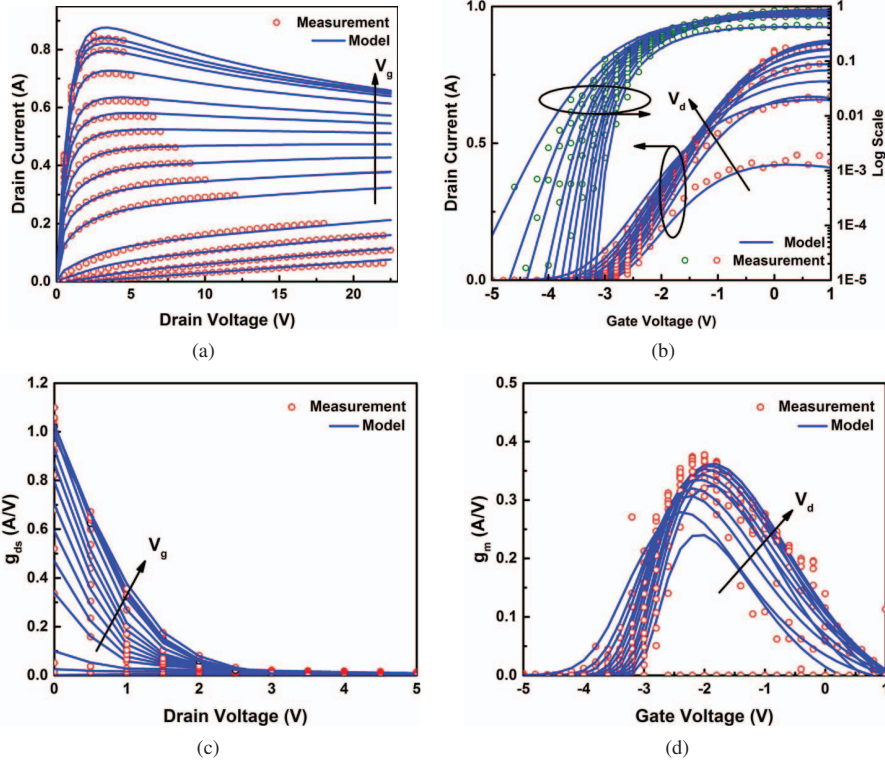


Fig. 1: Comparison between experimental and modeled data. (a), (c) $I_{ds} - V_{ds}$ and $g_{ds} - V_{ds}$ respectively for $V_{gs} = -3.2V$ to $1V$ in steps of $0.2V$ and (b), (d) $I_{ds} - V_{gs}$ and $g_m - V_{gs}$ for 12 different values of V_{ds} between $0.5V$ and $22.5V$.

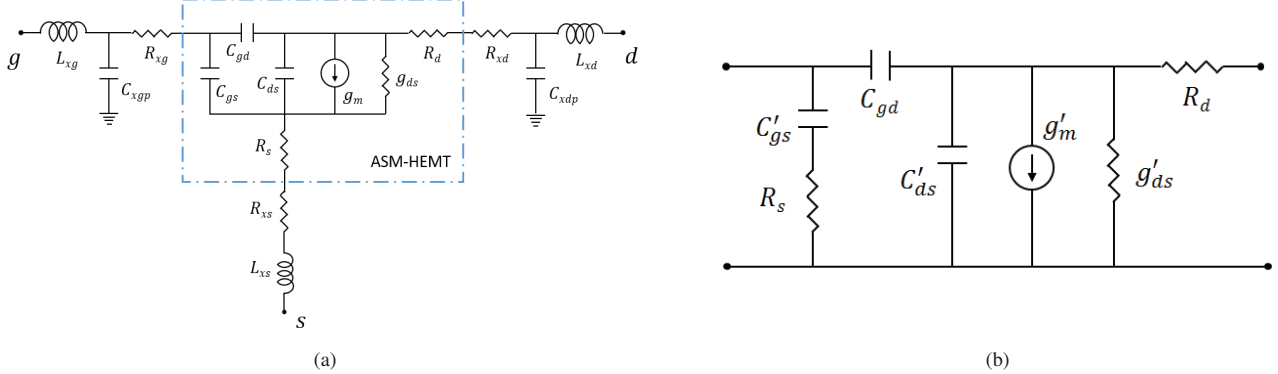


Fig. 2: (a) Small Signal Equivalent Circuit (SSE) Model of the device. The dashed region represents the intrinsic device as described by the ASM-HEMT model. The capacitances and the transconductance are calculated self-consistently from the surface potential [11]. Bias independent extrinsic elements are also shown. (b) SSE of the transformed intrinsic device with R_s absorbed as shown. g'_m , g'_ds , C'_gs and C'_ds are the intrinsic values divided by $1 + g_m R_s$.

The small signal equivalent circuit (SSE) representation of the device is shown in Fig. 2(a). C_{xgp} , C_{xdp} , R_{xg} , R_{xd} , R_{xs} , L_{xg} , L_{xd} and L_{xs} represent the bias-independent extrinsic parasitic elements that are introduced due to the device packaging, pads and contacts. In the SSE of the intrinsic device based on our model, C_{gs} , C_{gd} and C_{ds} represent bias-dependent intrinsic capacitances, g_m denotes the device transconductance whereas R_s and R_d denote access region resistances in the intrinsic device model [11]. All the intrinsic components are evaluated in terms of ψ . In Fig. 2(b), the SSE of intrinsic device is shown wherein R_s is absorbed and each one of C_{gs} , C_{ds} , g_{ds} and g_m gets divided by a factor of $1 + g_m R_s$ and updated to C'_{gs} , C'_{ds} , g'_ds and g'_m respectively. Both the input and the output ports are terminated with characteristic impedance (Z_0).

The intrinsic output impedance ($Z_{out,i}$) evaluated for this SSE is given by (2), shown in the beginning of the next page, where R_g is the gate resistance. This expression reduces to (3) and (4) under low and high frequency approximations, in which the effects of various elements are ignored depending upon the frequency. A careful examination of these approximate expressions reveals that they attain the form $Z_{out,i,low} = r + \frac{1}{j\omega C}$ and $Y_{out,i,high} = (Z_{out,i,high})^{-1} = (g + j\omega C)$ respectively leading to the formation of the kink [3]. S_{22} can now be calculated in terms of $Z_{out,i}$ as

$$S_{22}(s) = \frac{Z_{out,i} - Z_0}{Z_{out,i} + Z_0} \quad (1)$$

$$Z_{out,i}(s) = \frac{1}{g'_{ds} + sC'_{ds} + \left(\frac{sC_{gd}}{\frac{1}{Z_0+R_g} + \frac{sC'_{gs}}{1+sC'_{gs}R_s} + sC_{gd}} \right) \left(\frac{g'_m + sC'_{gs}}{1+sC'_{gs}R_s} + \frac{1}{Z_0+R_g} \right)} \quad (2)$$

$$Z_{out,i,low}(s) = \frac{1}{g'_{ds}} + \frac{Z_0 + R_g}{g'_m(Z_0 + R_g) + 1} + \frac{1}{sC_{gd}(g'_m(Z_0 + R_g) + 1)} \quad (3)$$

$$Y_{out,i,high}(s) = \frac{1}{Z_{out,i,high}(s)} = g'_{ds} + g'_m \left(\frac{C_{gd}}{C'_{gs} + C_{gd}} \right) + s \left(C'_{ds} + \frac{C_{gd}C'_{gs}}{C'_{gs} + C_{gd}} \right) \quad (4)$$

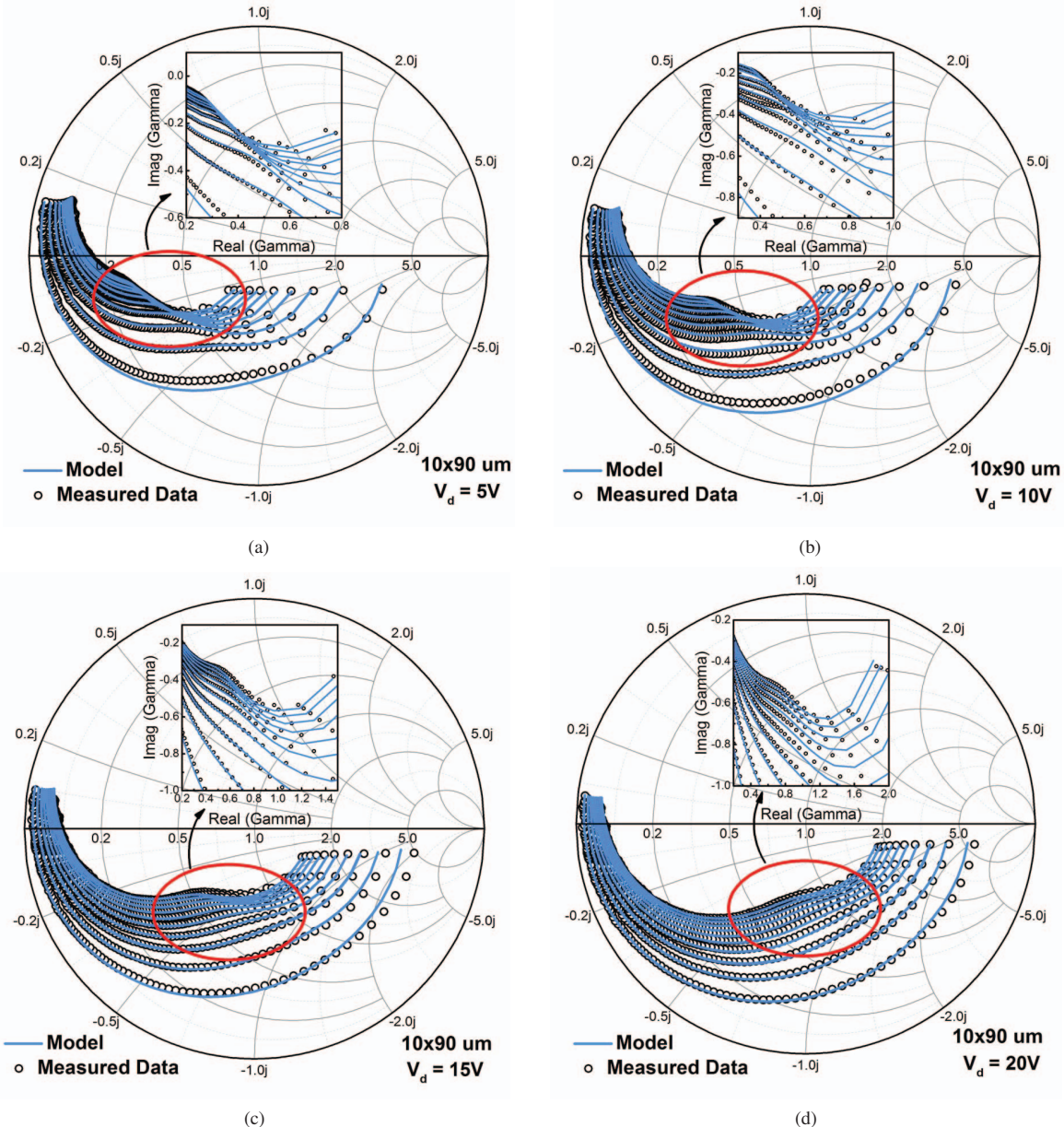


Fig. 3: Broadband Smith-Plots of S_{22} for a frequency range of 500 MHz to 50 GHz for a GaN device with gate periphery $10 \times 90 \mu\text{m}$. Results are shown for four different V_d values (a) 5V (b) 10V (c) 15V (d) 20V, each with ten V_g values (Outer contours: 10 mA/mm, Inner Contours: 100 mA/mm). The kink-effect is more pronounced as V_g increases, which is due to higher g_m for higher V_g , as long as self heating does not happen. With increasing V_d , the kink loses prominence due to a corresponding decrease in C_{gd} with drain bias. The measured and modeled results are in excellent agreement. Insets are added for better clarity of the region of interest.

IV. RESULTS AND DISCUSSION

We have implemented the model formulations in Verilog-A and performed simulations in Keysight's ADS circuit simulator. S-parameter measurements for a Qorvo GaN device with a gate periphery $10 \times 90 \mu\text{m}$ and gate length $L = 125 \text{ nm}$ are used for model validation. Measurement, carried out with a source excitation level of -13 dBm , in the form of .s2p file format are loaded into the ADS simulator. In the S-parameter simulation setup, .s2p components are appended at the gate and drain terminals of the device which correspond to error coefficients due to Thru Reflect Line (TRL) mode of calibration.

The S-parameters are simulated from 500 MHz to 50 GHz. Standard practice of small-signal parameter extraction is followed as proposed by Dambrine *et al.*. Fig. 3 shows an extensive comparison of the measured and modeled results for S_{22} of the $10 \times 90 \mu\text{m}$ device for 40 different bias conditions - 4 different values of drain voltage V_d (5V to 20V) with 10 different values of gate voltage V_g ($I_{ds} = 10$ to 100 mA/mm) for each value of V_d .

In each of the sub-plots, the kink-effect gains prominence as V_g is increased. This is primarily due to an increased values of g_m for higher V_g . Moreover, the Z_{out} on the Smith-chart corresponding to the kink frequency shifts towards the short circuit load as V_g increases which is due to a strong increase in the drain conductance (g_{ds}) with increasing V_g . As V_d is increased and keeping V_g fixed, the kink starts to diminish since the gate-drain capacitance C_{gd} follows a decreasing trend. The accurate modeling of the kink-effect with various bias conditions emphasizes the accuracy of bias dependence of the modeled device characteristics such as the transconductance and the intrinsic capacitances that are instrumental in determining the Z_{out} and therefore the kink in S_{22} as well.

V. MODELING OF KINK-FREQUENCY

Fig. 4 gives the measured and modeled values of the kink-frequency (f_K), as obtained from the smith plots, as a function of operating current (I_d). An interesting observation to be made is that f_K increases as I_d is increased. This characteristic is of interest particularly to RF Power Amplifier designers, since the model predicts suitable bias conditions to operate at such that the kink can be avoided. This property can be exploited to design output matching networks without the complexity which would otherwise be present due to the kink.

VI. CONCLUSION

We presented a physics-based model capable of predicting the kink observed in the S_{22} Smith-plot of GaN HEMTs. A thorough validation in a multi-bias setup was extensively performed with measured data for a GaN devices with gate periphery $10 \times 90 \mu\text{m}$ and an excellent agreement between measured and modeled results was obtained. Our results for the changing behaviour of the kink with respect to changing bias conditions advocate the strong accuracy in the modeling of the intrinsic device characteristics that play an important role in determining the kink in S_{22} .

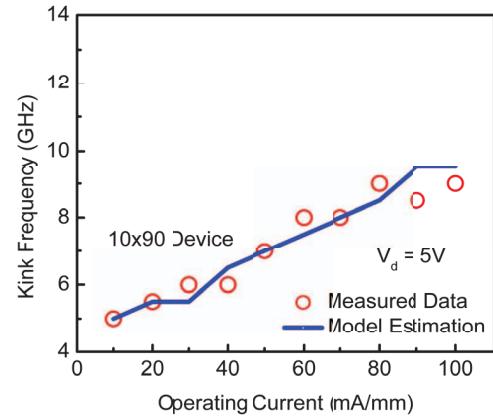


Fig. 4: Measured and modeled values of f_K as a function of V_g for $V_d = 5\text{V}$. The values are obtained directly from the Smith plots. f_K increases as I_d is increased.

ACKNOWLEDGMENT

This work was funded by Ramanujan fellowship research grant, Science and Engineering Research Board and Indian Space Research Organization.

REFERENCES

- [1] U. K. Mishra, *et al.*, "GaN-Based RF Power Devices and Amplifiers," *Proc. IEEE*, vol. 96, no. 2, pp. 287-305, Feb. 2008.
- [2] R. S. Pengelly, *et al.*, "A Review of GaN on SiC High Electron-Mobility Power Transistors and MMICs," *IEEE Trans. Microw. Theory Tech.*, vol. 60, no. 6, pp. 1764-1783, Jun 2012.
- [3] S.-S. Lu, *et al.*, "The Origin of the Kink Phenomenon of Transistor Scattering Parameter S_{22} ," *IEEE Trans. Microw. Theory Tech.*, vol. 49, no. 2, pp. 333-340, Feb 2001.
- [4] H-Y. Tu, *et al.*, "An analysis of the anomalous dip in scattering parameter S_{22} of InGaP-GaAs heterojunction bipolar transistors (HBTs)," *IEEE Trans. Electron Devices*, vol. 49, no. 10, pp. 1831-1833, Oct 2002.
- [5] G. Crupi, *et al.*, "An Extensive Experimental Analysis of the Kink Effects in S_{22} and h_{21} for a GaN HEMT," *IEEE Trans. Microw. Theory Tech.*, vol. 62, no. 3, pp. 513-520, Mar. 2014.
- [6] G. Crupi, *et al.*, "Kink Effect in S_{22} for GaN and GaAs HEMTs," *IEEE Microw. Wireless Comp. Lett.*, vol. 25, no. 5, pp. 301-303, May 2015.
- [7] A. Raffo, *et al.*, "Nonlinear dispersive modeling of electron devices oriented to GaN power amplifier design," *IEEE Trans. Microw. Theory Tech.*, vol. 58, no. 4, pp. 710-718, Apr. 2010.
- [8] S. Khandelwal, Y. S. Chauhan, and T. A. Fjeldly, "Analytical Modeling of Surface-Potential and Intrinsic Charges in AlGaN/GaN HEMT Devices," *IEEE Trans. Electron Devices*, vol. 59, no. 10, pp. 2856-2860, Oct. 2012.
- [9] S. Khandelwal, *et al.*, "Surface-Potential-Based RF Large Signal Model for Gallium Nitride HEMTs," *Proc. IEEE Compound Semiconductor Integrated Circuit Symp. (CSICS)*, pp. 1-4, 2015.
- [10] S. Khandelwal, "Compact Modeling Solutions for Advanced Semiconductor Devices," Ph.D. thesis, Dept. of Electron. Telecommun., Norwegian Univ. Sci. Technol., Trondheim, Norway, 2013.
- [11] S. Khandelwal, *et al.*, "Robust Surface-Potential-Based Compact Model for GaN HEMT IC Design," *IEEE Trans. Electron Devices*, vol. 60, no. 10, pp. 3216-3222, Oct. 2013.
- [12] S. A. Ahsan, *et al.*, "Capacitance Modeling in Dual Field-Plate Power GaN HEMT for Accurate Switching Behavior," *IEEE Trans. Electron Devices*, vol. 63, no. 2, pp. 565-572, Feb. 2016.
- [13] S. D. Mertens, "Status of the GaN HEMT Standardization Effort at the Compact Model Coalition," *Proc. IEEE Compound Semiconductor Integrated Circuit Symp. (CSICS)*, pp. 1-4, 2014.
- [14] G. Dambrine, *et al.*, "A New Method for Determining the FET Small-Signal Equivalent Circuit," *IEEE Trans. Microw. Theory Tech.*, vol. 36, no. 7, pp. 1151-1159, Jul 1988.